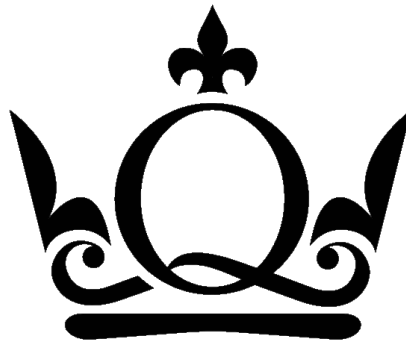# General Notes On Physics

Yuanpeng Zhang

March 28, 2016

School of Physics and Astronomy

Queen Mary, University of London

This page intentionally left blank.

Introduction

As a PhD student major in physics or probably those from any other subjects, focusing on experiments or learning specific techniques may not be the most important thing, although they seem to be. At the beginning of the PhD study, if there were someone saying something similar to me (actually, indeed there was someone – our dear Prof. Martin Dove), I would not agree with him/her in my deep mind (and, that's also indeed the case, sorry Martin). However, with the ongoing of the PhD research and study, I gradually came to realize that it is actually through continuous reading and summarizing (unfortunately, not working after working) that people (including myself) come up with new ideas. In another word, research is seems to be not about doing but rather thinking (through reading and writing). Then how do people think? Perhaps even the most smart guy in the world (like, Einstein) will never think of anything elegant all by him/herself. Imaging if without the hot discussion about the contradictory results for the experiments involving light in the late 19th centuary, how would it be possible for Einstein to come up with the seemingly crazy ideas about the theory of relativity. Maybe if without the famous Michealson-Morley experiments and all the other related exploration by lots of physicists, there would never exist the year of Einstein. Then how did Einstein know that people were confused with the strange behaviour of light? Maybe he heard of it from colleages, or maybe he read it from any reports. Anyway, there is no doubt that he need to communicate, somehow, with others. Reading, writing, listening, speaking, or comprehensively, communication, is the very first step that a child get to know the surroundings. This should be definitely also true for researchers and research work, whose task is just to know about the world we are living in and to reveal the mystery behind the scence as best as we can. After all, the real research is something about idea. Through reading, we could know the idea from others, and by writing we tell people how we understand matters and if fortunate, we may come up with some ideas about the problems proposed by others and share with the community for groups of experts to determine whether the idea does makes sense or not – that's just the point of publication.

Back to specific problems, in this article, the general introduction and some basic understanding of specific topics will be given. Basically, they are just the notes taken based on the reading of the most basic ideas of corresponding topic. The purpose of this article is for knowledge backup and storage. In another word, the article is about the most fundamental physics behind specific technique or method and its application. So it was hoped that this article can serve as the *minimum* preparation to learn something that is not our major. Such *minimum* preparation could help better understanding what people are doing using their main techniques (those may be unfamiliar to us). And only based on understanding what people are really doing can it be possible for us to sort out what may be helpful for our own research work or solving our specific problems. Based on such an idea, the discussion in this article will not go into details about any specific topics, but keeping the basic spirit of *minimum*.

Chapter 1

Spectroscopy

This chapter is about the basics of spectroscopy such as absorption spectroscopy, emission spectroscopy, scattering spectroscopy, etc. Briefly, spectroscopy is about the detection and explanation of the response with respect to the energy. By understanding the mechanism behind the experimental phenonema of specific spectroscopy, we may utilize spectroscopy to help us determining the properties (e.g. structural, optical and electrical properties, etc.) and also probably the depence of those properties for our materials.

1.1   Photoluminescence

- Radiative rate

  The *radiative rate* in this context is nothing to do with the nuclear reaction but rather is concerned about the photo emission from molecule or semiconductor after they have been excited by the incoming photons. When the energy of the incoming photon meets the gap of the material, the photons can be absorbed and correspondingly the electron will be excited from the ground state to the excited state. Since the excited state is higher in energy as compared to the ground state (that's just what 'ground state' means), the excited electrons tend to jump back to the ground state to lower the energy of the system. Briefly, there are two basic ways of decay – the radiative decay and non-radiative decay. The so-called radiative decay means the decay process is concomitant with the following light emission, which is given the name of photoluminescence. The radiative rate refers to the number of photons emitted per unit period (time), and it is also called the rate of spontaneous emission. Theoretically the radiative rate is described by the Fermi's golden rule, and here is the expression:

  $$\Gamma(\omega) = \frac{\omega^3 |\mu_{12}|^2}{3\pi\epsilon_0 \hbar c^3} = \frac{4\alpha\omega^3 n |\langle 1|\mathbf{r}|2\rangle|^2}{3c^2} \tag{1.1}$$

  where ω is the emission frequency, n is the index of refraction, ϵ_0 is the vacuum permittivity, $\hbar$ is the reduced Planck constant, c is the vacuum speed of light, and α is the fine structure constant. Equation -(1.1) indicates that if theoretically the initial and final state wavefunction can be determined, the corresponding radiative transition rate (radiative rate) can then be obtained. Here it should be noted that by far we are only concerned about the radiative decay - how many photons were emitted and how long the process takes, which then gives the radiative rate. As for how many photons were previously absorbed and furthermore how many photons were shined on the material, they are not what radiative rate concerns about. Instead, we have the notation of quantum yield to take care of those topics, which will be given in
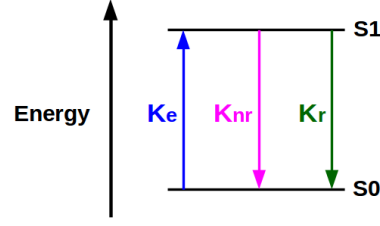
Figure 1.1: The illustration for photon absorption and decay.

the part of Quantum Yield. At last, it should also be pointed out that the introduction given here about radiative rate is based on the corresponding Wikipage.

- Quantum Yield

As discussed in the part of Radiative Rate, it has already been given that once the electron is excited to the excited state, it has two different ways to decay back to the ground state – radiative and non-radiative (see Fig. 1.1). Fig. 1.1 gives a simple sketch for the whole photons absorption and decay (including radiative and non-radiative decay) process, where K_e, K_r and K_{nr} represents the photon absorption, radiative decay and non-radiative decay, respectively.

Basically for application of the photoluminescence, we want as many radiative decay (which then emits light) as possible with the same amount of light being absorbed. To measure the weight of radiative decay takes among the whole decay, the notation of quantum yield is given as:

$$\Phi = \frac{Number\ of\ photons\ emitted}{Number\ of\ photons\ absorbed} \tag{1.2}$$

Using the notation used in Fig. (1.1), the quantum yield can be written down as:

$$\Phi = \frac{K_r}{K_r + K_{nr}} \tag{1.3}$$

By rearranging (1.3), we could have:

$$K_r = \Phi(K_r + K_{nr})$$
$$= \frac{\Phi}{\frac{1}{K_r + K_{nr}}} \tag{1.4}$$

Since $(K_r + K_{nr})$ together denotes the total decay rate – that means in one second (assuming SI unit) we have $(K_r + K_{nr})$ photons decaying. In the later discussion about the fluorescence lifetime, it will be given that the lifetime is actually defined as the reciprocal of $(K_r + K_{nr})$, i.e.:

$$\tau = \frac{1}{K_r + K_{nr}} \tag{1.5}$$

Then we have the following equation:

$$K_r = \frac{\phi}{\tau} \tag{1.6}$$

which can be used to determine the radiative rate, experimentally [1]. Before the end of this part, there are two things to point out. The first is about the non-radiative decay. The non-radiative decay is mainly due to the energy loss of the photo electron through the interaction with the phonon, i.e. the photo electrons transfer part of their energy to the vibration of lattice, which is, of course, non-radiative. Fig. 1.2
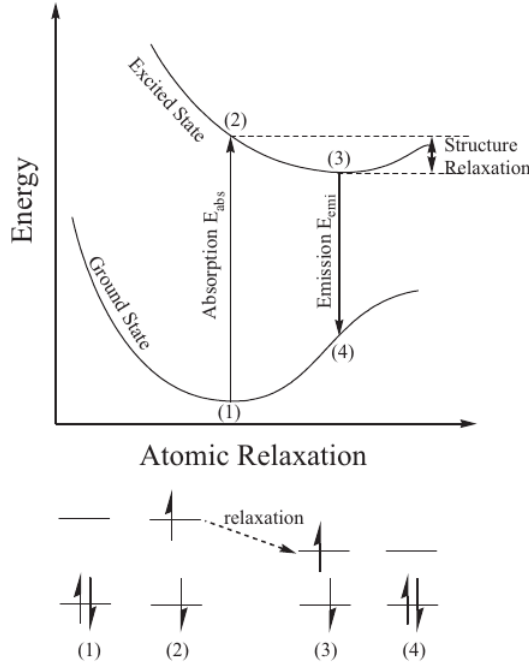
Figure 1.2: Schematic energy diagram of the ground state and the first excited singlet state of silicon nanoparticles. [2]

illustrates such idea. The second thing is about the internal/external quantum yield. Basically, the internal quantum yield concerns about the radiative emission as compared to the absorbed photons. While the external quantum yield takes care of the ratio of radiative emission compared to all the incoming photons shining on the material in question.

- Photoluminescence Lifetime

In the previous discussion about photoluminescence, it was given the notation of decay rate which concerns about how fast the excited system will decay to its ground state, accompanied either by radiation or not. However, in the above discussion it was not given the specific mathematical form involving the decay rate. Here in this part, the corresponding mathematical expression concerning the decay of the excited fluorophores and furthermore the definition of lifetime will be given. First of all, the general expression describing the behaviour of an excited population of fluorophores is given as:

$$\frac{dn(t)}{dt} = -Kn(t) + f(t) \tag{1.7}$$

where $n(t)$ is the number of excited elements at time t, K is the rate constant of all deexcitation processes and $f(t)$ is an arbitrary function of the time, describing the time course of **excitation**. If the excitation is switched off once the measurement for the number of excited elements start off, we should have $f(t) = 0$ for $t > 0$. Then (1.7) becomes:

$$\frac{dn(t)}{dt} = -Kn(t) \tag{1.8}$$

Solving equation-(1.8) will give us:
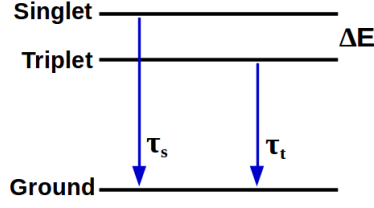
$$n(t) = n(0)exp(-Kt) \tag{1.9}$$

Figure 1.3: Illustration for the PL lifetime temperature dependence model. [3, 4, 5]

And here comes the definition of lifetime – τ of the fluorescence process:

$$\tau = \frac{1}{K} \tag{1.10}$$

which is just the form used by (1.5). And it could be noticed that in (1.5), the total decay rate K is separated explicitly into the radiative contribution K_r and the non-radiative part K_{nr}. Furthermore, based on the definition of lifetime (1.10), (1.9) can be rewritten as:

$$n(t) = n(0)e^{-t/\tau} \tag{1.11}$$

from which the importance of the definition of lifetime is clear: it measures the time it takes for the number of excited elements to decay to $1/e$ or 36.8% of the original population. Here it should be pointed out that the above discussion about the fluorescence lifetime is summarized based on the material given by: Click Me.

Given the definition of lifetime, it should also be mentioned that the application of fluorescence lifetime imaging – by measuring the lifetime of the molecule (e.g. one of the ways for lifetime imaging is through pixel-by-pixel lifetime measurement), it can yields information about the molecular microenvironment of a fluorescence molecule. Factors such as ionic strength, hydrophobicity, oxygen concentration, binding to macromolecules, and the proximity of molecules that can deplete the excited state by resonance energy transfer can all modify the lifetime of a fluorophore. Measurements of lifetimes can therefore be used as indicators of these parameters. For detailed information about the importance and advantages of lifetime imaging, and also about the corresponding measurement techniques, refer to the following materials: Material-1 & Material-2.

The lifetime of the fluorescence depends on many factors as given in the above paragraph, and there is another important factor that is material and environment independent – temperature. As an example, the temperature dependence of the PL for silicon nanostructures is often well fitted by the model proposed by Calcott *et* al [3, 4]. In this model (see Fig. 1.3), the excitonic levels are split by energy ΔE due to teh exchange interaction of an electron and a hole. The lower (upper) level is a triplet (singlet) state with a radiative lifetime τ_t (τ_s) as shown in Fig. 1.3. The overall temperature dependence of the PL lifetime can be calculated based on the Boltzmann statistics with a weighted factor of 3 for the triplet state (probably, accounting for the degeneracy 3 of the triplet state) and is described as:

$$\frac{1}{\tau} = \frac{\frac{3}{\tau_s} + \frac{1}{\tau_s}exp\left(-\frac{\Delta E}{k_B T}\right)}{3 + exp\left(-\frac{\Delta E}{k_B T}\right)} \tag{1.12}$$

where k_B and T are the Boltzmann constant and temperature, respectively. Here all the discussion about the lifetime model for Si nanoparticles comes from the following reference: [5].
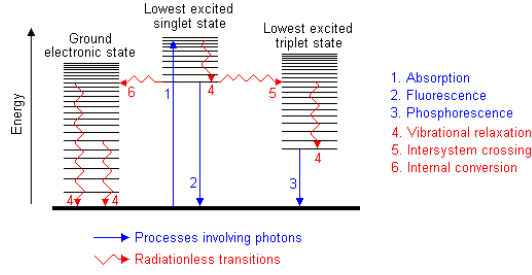
Figure 1.4: Illustration for different pathways of photoluminescence.

Another example is about the poor optical performance of Ge as a light emitter as discussed in Ref. [6]. The PL intensity $I(t)$ can be expressed as a function of time:

$$I(t) = B_1 e^{-t/\tau_1} + B_2 e^{-t/\tau_2} \tag{1.13}$$

where B_1 and B_2 are contants to be fitted for specific experimental results. τ_1 and τ_2 are the value of lifetime corresponding to two parts of the PL decay curve. In Ref. [6], the value of τ_2 was taken as the 'real' lifetime of Ge. Also in Ref. [6], it was also discussed the relationship between radiative recombination rate lifetime (τ_r), non-radiative recombination (τ_{nr}) and the quantum yield (ϕ). First the effective lifetime τ_t can be linked up with the radiative recombination lifetime τ_r and non-radiative recombination lifetime τ_{nr}:

$$\frac{1}{\tau_t} = \frac{1}{\tau_r} + \frac{1}{\tau_{nr}} \tag{1.14}$$

Therefore the quantum yield ϕ can be calculated:

$$\phi = \frac{1/\tau_r}{1/\tau_t} = \frac{1/\tau_r}{1/\tau_r + 1/\tau_{nr}}$$
$$= \frac{1}{1 + \tau_r/\tau_{nr}} \tag{1.15}$$

Before ending this part, there is one point to clarify: the notation of *fluorescence* and *photoluminescence*. Basically, fluorescence can be thought of as a specific form of photoluminescence. And the following quotation explains quite well about the distinction between the notation of photoluminescence and fluorescence:

> ",'
>
> *Photoluminescence, which occurs when the excited electron returns to its initial state in different wavelength. If this return process is radiative, it emits a photon whose energy gives the difference between the excited and the initial state energies. The emission spectrum shows a fingerprint peak related to the energy of each excited level.*
>
> *Depending on the time of Photoluminescence occurence and the sort of involved states, the processes can be divided to 2 main regime. 1: Fluorescence. 2: Phosphorescence.*
>
> ",'

The above quotation was initially given by the ResearchGate Question-answering. Also the correponding webpage has been clipped to '.pdf' file which can be found following the link: Click Me. And Fig. 1.4 shows all the possible pathways for the photoluminescence process, in which we can find that fluorescence is just one of them. It should be

clarified that for the discussion in thi article, if the general properties (e.g. the lifetime, etc.) are discussed, the difference between the notation usage (photoluminescence or fluorescence) will not be addressed, i.e. they are regarded as 'the same' when talking about the general properties of the photoluminescence system.

- Non-exponential Decay

In the part discussing photoluminescence lifetime, the decay of the excited states was thought of as exponential - see (1.9) and (1.11). However, in some certain circumstances, the decay of the excited states may not be well accounted by pure exponential behaviour. Delerue et al. [7] proposed that the non-exponential nature of the decay could be an inherent character of quantum confined indirect gap nanostructures [8]. The stretched exponential empirical law [9, 10] can be used to evaluate the general non-exponential decay timescale:

$$I(t) = I_0 e^{-(t/\tau)^\beta} \tag{1.16}$$

where I_0 is the initial PL intensity, τ the carrier lifetime and β the non-exponential parameter. The report from Derr et al. [8] corroborates this model.

- Temperature Dependence

The dependence of carrier recombination energy (i.e. the PL peak energy) as a function of temperature can be described using the Varshnis ad hoc equation [11]:

$$E_{gap}(T) = E_0 - \frac{\alpha_\nu T^2}{\Theta_D + T} \tag{1.17}$$

where E_0 is the peak position energy at $T = 0\ K$, Θ_D the Debye temperature of the material and α_ν a parameter related to the material. Again, the model was used in the report by Derr et al. [8], proving its applicability.

Here is the classical Arrhenius model for the temperature dependence (which is multiple exponential) of photoluminescence intensity [12]:

$$I(T) = \frac{1}{1 + C_1 exp(\frac{-E_{A1}}{k_B T}) + C_2 exp(\frac{-E_{A2}}{k_B T})} \tag{1.18}$$

where $I(T)$ represents the normalized integrated PL intensity. The parameters C_1 and C_2 are two constants related to the density of non-radiative recombination centres in the samples. E_{A1} and E_{A2} are the activation energies corresponding to the non-radiative recombination process. k_B is Boltzmann constant.

And the single exponential temperature dependence is given as (Click Me to achieve the file):

$$\frac{I(T)}{I_0} = \frac{1}{1 + C exp(-E_A/k_B T)} \tag{1.19}$$

where E_A is the activation energy, $I(T)$ is the photoluminescence intensity at temperature T, I_0 is the photoluminescence intensity at absolute zero temperature, and C is a constant (with the same meaning as it is in the multiple exponential model given above).

- Effective Mass Approximation (EMA)

The effective mass approximation (EMA) was first introduced in the model accounting for size effect in confined excitons by Efros et al. in 1982 [13]. The size effect is often termed as quantum confinement effect, which means the variation of the band structure of nanostructures due to the change in size (e.g. the reduction of bandgap with the decreasing of nanoparticles size), when the size of the nanoclusters is comparable to the corresponding Bohr exciton radius of the material. By applying the effective mass approximation, Efros et al. derived the energy shift due to the size effect is given by:

$$\Delta E = \frac{\hbar^2 \pi^2}{2\mu R^2} \tag{1.20}$$

where μ is the reduced mass of the material and R is the radius of the nanocluster. Here it should be mentioned that the model based on EMA also assumes spherical microcrystallites with infinite potential barriers at the crystal boundary, and the radius is replaced with teh average crystal size. Specifically for silicon bulk system, Brus [14] and Kayanuma [15] extended the simple model by introducing the Coulomb term and Rydberg energy. Therefore the bandgap as a function of radius of silicon bulk material is given by:

$$E(R) = E_g + \frac{\hbar^2 \pi^2}{2R^2} \left(\frac{1}{m_e^* + m_h^*} \right) - \frac{1.786 e^2}{\epsilon_r R} + 0.284 E_R \tag{1.21}$$

where $1.786 e^2 / \epsilon_r R$ is the Coulomb term and $0.284 E_R$ gives spatial correlation energy with a minor correction. In practice, the model based on EMA may or may not work well depending on the specific system and nanocluster composition (e.g. whether interface effect exists, etc.). [16]

- Phonon Replica

  The direct recombination of exciton (electron and hole pair) always happen at the band edge - conduction band (or other intermediate band) bottom to valence band top (See General Notes On Semiconductor Physics summary). The momentum conservation requires the photon involved in the direct recombination process should be approximately with zero momentum. In another word, The electron and hole involved in the recombination should be approximately with identical momentum. However in some cases, the phonons may also get involved in the exciton recombination process. In such processes, for electrons (holes) not at the bottom of the conduction band (the top of the valence band), they may pass part of their energy to phonons with certain energy instead of wasting the energy and directly go to the bottom (top) of the band. At the same time passing energy to the phonons, excitons also interchange momentum with phonons to get the zero energy necessary for the direct transition to emit photons. Therefore in such cases, the direction emission of photons (with the energy E_0) is accompanied by several other phonon-assited recombination, which is then given the name of *phonon replica*.
  Apart from the phonon replica accompanying the direct transition, there also possibly exists the fine structure of the recombination, which is connected to the polariton effects. Briefly, the exciton polariton refers to the quanta (discrete energy level) formed due to the splitting of energy level between longitude (LO) and transvere (TO) polarization.
  For details about the discussion, see the following link, which is extracted from the book - *The Physics of Semiconductors - An Introduction Including Devices and Nanoparticles* by Marius Grundmann: Click Me.

- Radiative lifetime model

The radiative lifetime can be written as [17]:

$$\frac{1}{\tau_{rad}} = \frac{3e}{8\hbar c}\sqrt{\epsilon}\,\omega\Big(\frac{P}{\hbar c}\Big)^2 I \tag{1.22}$$

where ω is photon frequency, ϵ the dielectric susceptibility of the host medium, and P rhe optical interband matrix element describing the contribution from the Bloch functions (Thinking about the Fermi's golden rule). And the term I characterizes the overlap integral between the electron and the hole wave functions, which was assumed to be unity in its original form [18].

1.2   Raman Spectroscopy

- Quantum confinement Model for Raman

The Raman Spectroscopy gives the information about the phonon modes in the material. When the size of the material is down to where the quantum confinement starts to take the effect (roughyl, on the magnitude of nanometer), the intensity of the Raman peak can be described with specific model which links up the size of the material and the Raman scattering intensity. Here are given two commonly used models describing the size-dependence of the Raman scattering intensity. [19] The first one describes the wave vector relaxation related to the finite-sized nanocrystal effect:

$$I_1(\omega) \propto \int_0^1 exp\Big(\frac{-q^2L^2}{4}\Big)\frac{d^3q}{[\omega-\omega(q)]^2+[\Gamma_1/2]^2} \tag{1.23}$$

where a Gaussian spatial correlation function $exp(-q^2L^2)/4$ accounts for wave vector relaxation related to the finite-sized nanocrystal effect and structural disorder. And q refers to the wave vector, $\omega(q)$ is the phonon dispersion function, Γ_1 is the full-width at half maximum (FWHM) and inversely proportional to the intrinsic phonon lifetime, L is the diameter of the correlated QDs.
The second model is given as:

$$I_2(\omega) \propto \frac{\Gamma_2}{[\omega-\omega(q)]^2+[\Gamma_2/2]^2} \tag{1.24}$$

which accounts for the homogeneous broadening caused by particle/matrix coupling. And all the symbols in equation-1.24 represents the same quantity as they are in equation-1.23.
It should be mentioned that the model as given above may encounter problems when describing particles with quite small size (e.g. ¡ 5 nm). corresponding discussion about the problem Can be found in our published JSR paper and the following resopnse letter to referees when submitting the paper: Click Me.
First of all, the size extracted from fitting Raman spectra (based on the above mentioned phonon confinement model) may or may not correspond to the real particle size, which can actually include, but not limited to, twins, stacking faults, inclusions, vacancies, boundaries and pores [20]. And generall the size fitted from Raman spectra corresponds to the so-called 'coherent length'. Some reports show that the coherent length is consistent with the nanoparticle real size [21], while some refers the coherent size to the spacing between defects or impurities. [22]

Another aspect is that the phonon confinement model assumes uniform size and shape, and in Will's thesis, a model which contains the shape variance correction was introduced. For details and corresponding reference about the corrected model, refer to section 3.4.2 following the above given link for Will's thesis. Here is given the theoretical model:

$$I(\omega) = \int \rho(L) dL \, I_0 \int \frac{d^3 |C(0,q)|^2}{[\omega - \omega(q)]^2 + (\Gamma_0/2)^2} \qquad (1.25)$$

where $\rho(L)$ is the long-normal size distribution which corresponds to the density of vibrational states as each particl vibrates with a frequency that is inversely proportional to its size. The long-normal distribution is given by:

$$\rho(L) = A \, exp\left(\frac{-log(L/L_0)^2}{2\sigma^2}\right) \qquad (1.26)$$

where σ is a measure of the distribution width, L_0 is the size that corresponds to the maximum of the distribution and A is a constant. Furthermore, the surface phonon may become more significant as the nanoparticle size decreases, since the surface layer thickness does not change with the particle size changing. Also, if there is disordered region in the nanoparticles, the anisotropic properties may bring in distinctive phonon modes than that of crystalline part. All of these factors may lead to the failure of phonon confinement mode to detect the 'real' size of the nanoparticle in interest. For detailed discussion, see the section 3.4.3 and 3.4.4 in Will's thesis.

Chapter 2

Condensed Matter & Materials Physics

2.1 Crystallography

Crystallography basically concerns about the arrangement of atoms within solids and liquids, and the atomic vibrations dynamics within them. Beyond the structure (either local or long-range order), crystallography to large extent focuses on the link between the structure and the electronic structure, e.g. the energy band structure. Furthermore, such link between atomic arrangement and the electronic structure could serve as the bridge between the structure in crystallography and the optical or electric properties of materials. In this section, some crucial points about the crystallography will be introduced. Again, it should be repeated that no detailed introduction about each single point will be given, rather just some key understanding obstacles will be clarified instead.

- Maxwell Rule For Structure Stability

  The so-called Maxwell relationship given below is a simple tool for predicting whether some given structural configuration is stable or not, especially for those structure configuration problems involving defects. First of all from the perspective of energy, the potential energy connected with the chemical bonds is given by:

  $$V = \frac{1}{2} \sum_{i,j} \alpha(\Delta_{i,j})^2 + \frac{1}{2} \sum_{u,j,k} (\Delta_{i,j,k})^2 \qquad (2.1)$$

  Here the first term concerns about the energy associated with the bond length changing, and the second term reflects the energy connected with the bond angles changing. And the preferred configuration should be, certainly, connected with the energy minima based on equation-2.1. At zero temperature, the Maxwell relationship, which was deduced based on 2.1 is given as:

  $$M_0 = DN - N_c - (D + \alpha) \qquad (2.2)$$

  where $D = 1, 2, 3$ is the dimension of the solid, $N = \sum_{r=1}^{k} n_r$ with n_r as the number of atoms with coordination number r in the system. N_c is the number of constraints (angle/position) involved in the system and it is given as:

  $$N_c \equiv \left[\sum_{r=1} n_r \left(\frac{r}{2} \right) \right]_{bond} + \left[\sum_{r=1}^{k} n_r \left(\frac{D-1}{2} \right) (2r - D) \right]_{angle} \qquad (2.3)$$

In general, the system with $M_0 > 0$ is unstable, and those with $M_0 < 0$ is stable. Based on the system stability implied by the Maxwell relationship, it can be further extended that the unstable system (those with $M_0 > 0$) should not easily accommodate defects since the system is already by itself not stable. While for stable system (those with $M_0 < 0$), the system is prone to forming defects.

Details about the above discussion can be found in the following two references: Material-1 and Material-2.

2.2 Quantum Dots

This section will mainly focus on some general topics about the quantum dots (QDs), which is actually a big family with quite a few members such as metal QDs (Au, Ag, etc.), II-VI QDs (ZnS, ZnO, etc.), III-V QDs (InAs, GaAs, etc.) and group IV QDs (Si, Ge, C). Here in current context, the physical properties concerning the QDs will be highlighted. And before the introduction, an important question should be asked - what is QDs? Can all the materials with size down to 10 nm be called QDs? Actually, the answer is QD is a special case of nanocluster that is compromised of *semiconductors*.

- Quantum confinement

The confinement model

Here the confinement model based on the simple yet powerful effective mass model will be introduced. Since the core-shell QDs will
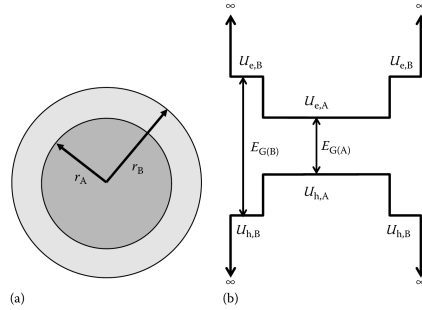

Figure 2.1: The illustration for (a) a spherical core-shell QD & (b) potential energy profile in a core-shell QDs.

be mainly based for the discussion in this section, therefore it should be mentioned that the simple effective mass model does not take the coupling between the conduction band (CB) and the valence band (VB) into consideration. First of all, the following basic form of the Shrödinger equation will be used:

$$\left[-\frac{\hbar^2}{2m_i} + V_i(\vec{r}) \right] \Psi_{n,i}(\vec{r}) = E_{n,i} \Psi(\vec{r}) \tag{2.4}$$

Here $i = e$ or h indicating the type of carrier, m_i is the effective mass of the carrier, and $V_i(\vec{r})$ represents the confinement potential, for which the illustration is given in Fig. 2.1. As mentioned above, the core-shell QD will be taken as the example for the discussion in this section, and corresponding confinement potential ($V_i(\vec{r})$) in equation-

2.4 is illustrated in Fig. 2.1. In mathematics, we have:

$$V_i(\vec{r}) = \begin{cases} U_{i,A} & 0 \le r < r_A \\ U_{i,B} & r_A \le r < r_B \\ \infty & r \ge r_B \end{cases}$$

In the equation above, $U_{i,A}$ and $U_{i,B}$ represent either the bottom of CB and or the top of VB in the core and shell regions, respectively. Thus, their difference $|U_{i,A} - U_{i,B}|$ represents the confinement potential of the ith particle. Here there are two aspects to point for better understanding of the confinement model. The first one is about the scale and ground potential in the core-shell model given above in Fig. 2.1. It should be clarified that the ground potential selection (i.e. at which level the potential energy is defined as zero) does not affect the discussion (mainly about the quantinization of the energy level in both of the core and shell regions given in the core-shell model) at all. If looking at the Schr*ödinger* equation given in 2.4, it can be easily imagined that if adding a constant (accounting for the floating ground potential level) on both sides, nothing will change except the absolute value of the eigen-energy. The other aspect is that all the discussion given above (and also as following) does not only apply to core-shell model, which means there is no problem for such model to work directly on the independent QD model, which is, actually, even more simple than the core-shell situation since we only have two different regions in the independent QD model.

Holding the Schrödinger equation and the well-defined potential in hand, it is then straightforward to solve the Schrödinger equation in different regions. Then considering the continuous condition of the wavefunction at the boundary of two adjacent regions in the model, also taking into account the normalization of the wavefunction in the whole space, the energy level in different regions (certainly, together with all the corresponding wavefunctions) can then be given specifically. For detailed discussion, the following book can be referred to: Handbook of Nanophysics: Nanoparticles and Quantum Dots (Section 35.4).
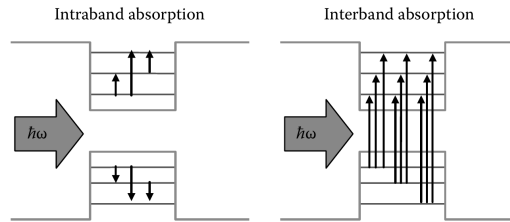

Figure 2.2: The discrete energy levels in the core region of the core-shell QD, together with the illustration for the different types of photons absorption in core-shell QDs, when illuminated by the light source with energy $E = \hbar\omega$

It is noteworthy that the energy levels finally obtained based on the discussion and formulation given above are discrete in either CB and VB in both the core and shell regions, which is basically where the quantum confinement effect is reflected - the quantinization of the energy band, which allows the further development of the application of QDs for opto-devices. In Fig. 2.2 the discrete energy levels within the core region is given. Once the discrete energy levels are generated in the QDs, it creates opportunities for the interaction with photons -

either absorption of the incoming photons or the emission of photons by the QDs themselves. As illustrated in Fig. 2.2, there are basically two different kinds of electronic transitions: intraband (Fig. 2.2 (a)) and interband (Fig. 2.2 (b)). And obviously, the interband transition is only possible when the energy of the incident photons is larger than the band gap energy of the material investigated.

Before going onto the next part of discussion about the eletrons/holes localization in either the core or hole region in the core-shell QDs, the quantinized energy levels in the core region of the core-shell QDs, or simply just the QDs for the independent QDs should be given:

$$E_{n,l}^{(e,h)} = \frac{\hbar^2 x_{n,l}^2}{2m_{e,h}R^2} \tag{2.5}$$

where $x_{n,l}$ represents the nth root of the spherical Bessel function $j_l(x)$ (the solution for the radial part of the Schrödinger equation while using the variable separation method). It can be obviously seen that the discrete energy levels does directly depend on the size of QDs - through the parameter R. For noninfinite confinement barriers, the size dependence becomes weaker $E_{n,l}^{(e,h)} \propto R^{-\alpha}$, where $1 < \alpha < 2$. From the discussion above, we should have already found that the discrete energy levels formulation applies to both the independent QDs and the core-shell QDs. And the only difference is that the confinement potential for independent QDs is infinite by assumption, while the confinement potential for the core region of the core-shell QDs model is nonfinite.

Electrons/Holes Localization

According to the solution of the wavefunction based on the effective mass model, the information about the electrons/holes localization in
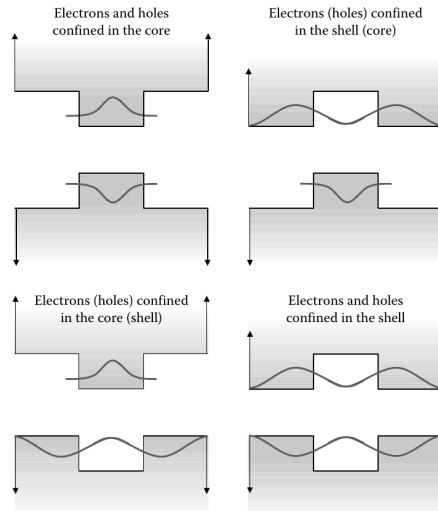
Figure 2.3: Possible band structure alignment in core-shell QDs.

different regions of the core-shell models can be obtained. Here the detailed solution of the electrons/holes wavefunctions will not be given, with only the graphic illustration for the electrons/holes localization provided in Fig. 2.3. In Fig. 2.3 it can be obviously seen the different types of electrons/holes localization in different regions of the core-shell QDs model. And basically the localization can be divided into two basic types according to whether the electrons and holes are

localized in the same region (type-I) or not (type-II). The important point here is the different types of electrons/holes localization leads to different binding energy between electrons and holes due to the different space separation. And such difference leads to different fortune of different types of core-shell QDs (e.g. type-I: CdSe/CdS & CdSe/ZnS, type-II: CdSe/CdTe) for applications such as the photovoltaics, etc. The thing is, as compared to independent QDs, the core-shell QDs provide more possibilities for the electrons/holes distribution in the QDs. Therefore in some configurations (e.g. the spatial separation of electrons and holes in type-II core-shell QDs is increased due to the confinement potential) the electrons and holes are further separated, which benefits the conversion of the photon energy to electrical energy.

Excitons

Once the electrons in the conduction band (either in the core or the shell region) are excited and the corresponding holes will then be formed. Then the generated electrons and holes within the QDs will natually interact with each other to form the so-called *exciton*. Taking into account of the binding energy of the exciton, the total energy of the exciton, in its simplest form, can be given as:

$$E_X = E_e + E_h + E_G - E_B \tag{2.6}$$

where E_e and E_h are the discrete energy states, obtained through solving the Schrödinger equation based on the effective mass model as discussed above, in specific regions of the core-shell QDs. E_G is the band gap of the materials. E_B is the exciton binding energy which can be obtained using the following formulation:

$$E_B = -\frac{e^2}{4\pi\epsilon_0\kappa} \int \int \frac{|\Psi_e(\vec{r}_e)|^2 |\Psi_h(\vec{r}_h)|^2}{|\vec{r}_e - \vec{r}_h|} d\vec{r}_e d\vec{r}_h \tag{2.7}$$

where $\epsilon_0\kappa$ is the dieletric constant of the material.

PS: *the exciton binding energy is simply given as:*

$$E_B = -\frac{\mu_{eh}}{\kappa} \times 13.6 eV \tag{2.8}$$

where $\mu_{eh}^{-1} = m_e^{-1} + m_h^{-1}$ and κ are the reduced mass and the dielectric constant of the material, respectively. And it is straightforward to understand equation-2.8 - since if imaging the generated hole after the electron excitation as the analogue to proton, then the electron-hole interaction is just simply a two-body problem which is analogue to the hydrogen atom. And the difference for the electron-hole interaction from that between electron and proton is that the proton can be thought of as infinitely heavy as compared to electron, which is however not the case for holes. Therefore the reduced mass is introduced in the formulation given in 2.8.

On the basis of equation-2.6, the exciton energy for different type of core-shell structure should be adjusted a bit accordingly. For example, the ground-state exciton energy $E_X^{(0)}$ for type-I (e.g. CdSe/CdS and CdSe/ZnS) and type-II (CdSe/CdTe) systems are, respectively, given by:

$$E_X^{(0)} = E_{G(CdSe)} + E_{1,0}^{(e)} + E_{1,0}^{(h)} + E_B \tag{2.9}$$

$$E_X^{(0)} = E_{G(CdSe)} - V_h + E_{1,0}^{(e)} + E_{1,0}^{(h)} + E_B \tag{2.10}$$

where the introduction of V_h term in 2.10 accounts for that electrons and holes are localized in different regions in type-II core-shell QDs,

and the barrier potential between the two regions (core and shell) should be considered. And it should be mentioned that details about the the evaluation of the exciton binding energy can be found in the above mentioned book (P_{35-11} - P_{35-12}).

Absorption & Photoluminescence

Once the incident photons are absorbed by the QDS, the concominant decay of the photoelectron to its original ground level will possibly bring the photoluminescence (PL, radiative decay). The corresponding PL is called the stimulated recombination (of electrons and holes). For obvious reason, the stimulated recombination is related to the absorption. Since the incident light is absorbed in creating e-h pairs, most of the excitations occur near the surface, restricted to a region within a diffusion length (or absorption length) of the illuminated surface. Moreover, the absorption and the following photoluminescence will also be accompanied by the self-absorption, which then leads to that the photoluminescence will not propogate far from the originally irradiated region (where the absorption happens). Therefore, most of the photoluminescence is subject to the irradiated side of the sample in experiment, which is often called the *front end photoluminescence*.

Link To Applications

As can be simply deduced from 2.5, the energy levels within the QDs (either the independent ones or the ones with core-shell configuration) can be tuned by the size of the QDs. In the above mentioned book, there are quite a few examples showing the size dependence of the electrons and holes energy, and also the exciton binding energy in the core-shell QDs. Also, it was shown (in the above mentioned book) that besides size control, covering QDs with another mateiral offers additional degrees of tuning QD electrnic properties. All of the capabilities of controlling the properties of QDs open up more possibilities of pursuing better performance of QDs on the application such as opto-sensors, photovoltaics, etc., through simply tuning the size, surface passivation, etc.

- Bandgap of QDs

According to the quantum confinement theory, the electrons and holes are spatially restricted by the surface potential barrier (which actually comes from the size effect). Therefore both the electrons and holes are more localized as compared to the situation for bulk materials. This increases the lowest energy related to the optical emission, which is, from the perspective of band theory, due to the increasing of the effective bandgap. Qualitatively, this can be understood as extra energy is needed to restrict (or, localize) the electrons or holes motion in space. In another word, the electrons and holes cannot move as 'freely' as they can in the bulk materials, which certainly needs some extra energy just based on the intuition.

The early theoretical description of the relationship between the QDs bandgap and the particle size was given by Efros in 1980s [23]:

$$E_n = E_g + \frac{h^2\pi^2}{2\mu R^2} \qquad (2.11)$$

where E_g is the bandgap of the bulk semiconductor, h Plank's constant, R the radius of the QDs, and μ the reduced mass of the exciton given by $m_e m_h/(m_e + m_h)$, and m_e & m_h are the masses of the electron and hole, respectively. Later, the formula was developed to include the Coulombic interaction and the correlation energy by Brus

and coworkers [23]:

$$E_n = E_g + \frac{h^2\pi^2}{2\mu R^2} - \frac{1.786e^2}{\epsilon R} + 0.284E_R \qquad (2.12)$$

where E_R is the Rydberg (spatial correlation) energy of the bulk semiconductor:

$$E_R = \frac{\mu e^4}{2\epsilon^2\epsilon_0^2 h^2} = 13.56\frac{\mu}{\epsilon^2 m_e} \qquad (2.13)$$

where ϵ_0 is the permittivity of free space, ϵ the dielectric constant of the bulk semiconductor, and m_e the mass of the electron.

- About Mie Theory

  The primary theory concerning the scattering interaction between small spherical particles and light was initially given by Mie in the early 1900s [23, 24]:

$$E(\lambda) = \frac{24\pi N_A r^3 \epsilon_m^{3/2}}{\lambda ln(10)}\Big[\frac{\epsilon_i(\lambda)}{(\epsilon_r(\lambda) + 2\epsilon_m)^2 + \epsilon_i^2(\lambda)}\Big] \qquad (2.14)$$

  where $E(\lambda)$ is the extinction (sum of absorption and scattering), N_A the density of the nanoparticles, r the radius of the nanoparticle, ϵ_m the dielectric constant of the metallic nanoparticle, λ the wavelength of absorbing radiation, and ϵ_i, ϵ_r are the imaginary and real parts of the λ-dependent dielectric function of the nanostructure. Furthermore, for non-spherical nanostructures, the denominator of the term in bracket of equation-(2.14) should be replaced by the following term:

$$(\epsilon_r(\lambda) + \chi\epsilon_m)^2 \qquad (2.15)$$

  where χ ranges from 2 (for perfect sphere) to 17 and beyond. [23, 25]

- Kubo Gap

  The Kubo gap is the average spacing that exists between consecutive energy levels. As the size of material in question decreases, the Kubo gap increases accordingly, and concominantly the density of states (DOS) at the Fermi level will decrease. The electrical conductivity (since here it is the consecutive band that matters, therefore we are actually focusing on metallic materials) and magnetic susceptibility are also both influenced by the Kubo gap and vary according to the size of the Kubo gap. For details about the Kubo gap, see the link here to Wikipedia.
  Here is the quantitative dependence of the Kubo gap on the size of nanostructures [23]:

$$\delta = \frac{3E_f}{2N} \qquad (2.16)$$

  where δ is the Kubo gap – energy spacing between adjacent E levels, N the nuclearity – the number of atoms in the nanocluster, and E_f is the energy of the Fermi level.

2.3   Band Theory

The quantum mechanics for solid crystalline structure, for which atoms are arranged periodically, leads to energy band theory. Assuming the potential varies with the same periodicity with that of the crystal, the so-called Bloch theorem can be deduced, based on which further discussions and models, including the nearly-free electron gas model, the tight binding model, etc.

can be carried out. One of the most important aspects of the band theory is the direct link set up between the band gap and the crystal potential. And such link can be deduced from either nearly-free electron gas model, the tight binding model and some other more complex models (i.e. electronic structure calculation models such as Hartreee-Fock method, DFT, etc.). Here in this article, a simple one-dimensional model will be introduced instead of focusing on those complicated method with tedious maths.

- Kronig-Penny Model

  Although the Kronig-Penny model, proposed in 1931 by Kronig and Penny [26], is a quite much simplified model (and also for one-dimension only), it does give reasonable explanation and thus a first impression on the band structure formed in the periodic crystalline material. The potential in the Kronig-Penny model is assumed to be an infinite periodic rectangle potential depicted in Fig. 2.4. There are two distinctive
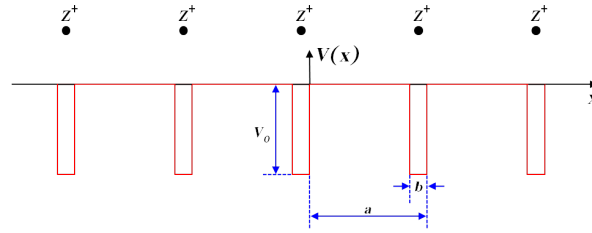

Figure 2.4: The illustration for the rectangle periodic potential assumed by Kronig-Penny model.

solutions of the Schrödinger equation for such rectangle periodic potential. For the region $0 < x < (a - b)$, the Schrödinger equation is given as:

$$-\frac{\hbar^2}{2m}\psi_{xx} = E\psi \tag{2.17}$$

where ψ_{xx} represents the second derivative of ψ over x. The general solution form can be given as:

$$\psi = Ae^{i\alpha x} + A^{'}e^{-i\alpha x} \tag{2.18}$$

where A and $A^{'}$ are two undetermined constants, and α is defined as:

$$\alpha^2 = \frac{2mE}{\hbar^2} \tag{2.19}$$

And for the second region $-b < x < 0$, the Schrödinger equation takes the form:

$$-\frac{\hbar^2}{2m}\psi_{xx} = (E + V_0)\psi \tag{2.20}$$

for which the general solution form is given as:

$$\psi = Be^{i\beta x} + B^{'}e^{-i\beta x} \tag{2.21}$$

where B and $B^{'}$ are two undetermined constants, and β is defined as:

$$\beta^2 = \frac{2m(E + V_0)}{\hbar^2} \tag{2.22}$$

According to Bloch theorem, the electron wavefunction in 1D periodic structure with the periodicity of a can be given in the following form:

$$\psi_{Bloch} = u(x)e^{ikx} \tag{2.23}$$

where the function $u(x)$ is the periodicity of a, i.e. $u(a+x) = u(x)$. To employ the periodic condition of the function $u(x)$, we need to find the form of $u(x)$ for each of the above two regions, for which the solution of Schrödinger equation is given in different forms. By manipulating 2.18 and 2.21, we have:

$$\psi(0 < x < a - b) = Ae^{i\alpha x} + A^{'}e^{-i\alpha x}$$
$$= e^{ikx} \cdot \left(Ae^{i(\alpha-k)x} + A^{'}e^{-i(\alpha+k)x}\right) \quad (2.24)$$
$$\Rightarrow u(0 < x < a - b) = Ae^{i(\alpha-k)x} + A^{'}e^{-i(\alpha+k)x} \quad (2.25)$$

Similarly,

$$u(-b < x < 0) = Be^{i(\beta-k)x} + B^{'}e^{-(\beta+k)x} \quad (2.26)$$

The following continuous conditions should be applied:

$$\psi(0^-) = \psi(0^+), \ \psi^{'}(o^-) = \psi^{'}(0^+) \quad (2.27)$$
$$u(-b) = u(a - b), \ u^{'}(-b) = u^{'}(a - b) \quad (2.28)$$

The above continuous conditions yield the following matrix equation:

$$\begin{bmatrix} 1 & 1 & -1 & -1 \\ \alpha & -\alpha & -\beta & \beta \\ e^{i(\alpha-k)(a-b)} & e^{-i(\alpha+k)(a-b)} & -e^{-i(\beta-k)b} & -e^{i(\beta+k)b} \\ (\alpha-k)e^{i(\alpha-k)(a-b)} & -(\alpha+k)e^{-i(\alpha+k)(a-b)} & -(\beta-k)e^{-i(\beta-k)b} & (\beta+k)e^{i(\beta+k)b} \end{bmatrix} \begin{bmatrix} A \\ A^{'} \\ B \\ B^{'} \end{bmatrix} = \begin{bmatrix} 0 \\ 0 \\ 0 \\ 0 \end{bmatrix} \quad (2.29)$$

For the equation above to have non-trial solution, the determinant of the matrix should be zero, which then finally leads to the following equation:

$$cos(ka) = cos(\beta b)cos[\alpha(a - b)] - \frac{\alpha^2 + \beta^2}{2\alpha\beta}sin(\beta b)sin[\alpha(a - b)] \quad (2.30)$$

To further simplify the expression and discuss the indication about the band structure, the following assumption is then made:

$$b \to 0, \; V_0 \to \infty, \; V_0 b = constant \tag{2.31}$$

Such assumptions then lead to the following relations:

$$\beta^2 b = constant, \; \alpha^2 b \to 0 \tag{2.32}$$

$$\beta b \to 0, \; sin(\beta b) \to \beta, \; cos(\beta b) \to 1 \tag{2.33}$$

Applying 2.31 to 2.33, the following expression then can be obtained:

$$cos(ka) = cos(\alpha a) - P\frac{sin(\alpha a)}{\alpha a}, \; P = \frac{mV_0 ba}{\hbar^2} \tag{2.34}$$

By inspecting 2.34, it can be found that the left-hand side is only the function of k while the right-hand side is only the function of E (see 2.19 for the relation between α and E). Therefore, the equation 2.34 determines the dispersion relation ($k - E$ relation), and furthermore we could see that the left-hand side should be always less than (or equal to) 1 while there is no such restriction for the right-hand side. This indicates that for some value of energy, there couldn't be found any real k value that satisfy the relation - 2.34 - thus explaining the bandgap.

All the above discussion is based on Wikipedia, refer to the link here.

2.4   Magnetic Property

- Magnetoresistance & Magnetic Reluctance

Basically magnetoresistance (MR) refers to the changing of electrical resistance when external magnetic field is applied. Early history of the magnetoresistance can date back to middle 19th century, and for detailed information about the introduction to magnetoresistance refer to Wikipedia: Click Me! Actually, it is the discovery of the giant magnetoresistance (GMR) that brings the MR effect to real application for which the typical examples is just the application in hard drive. Before going onto discuss the mechanism of the GMT phenomenon, there is one point to clarify about the notation of MR and the magnetic reluctance. On Wikipedia, the definition of magnetic reluctance is given as - *Magnetic reluctance, or magnetic resistance, is a concept used in the analysis of magnetic circuits. It is analogous to resistance in an electrical circuit, but rather than dissipating electric energy it stores magnetic energy.* (see the link). In English, there is nothing to clarify but for the Chinese translation, both magnetoresistance and magnetic resistance (or, reluctance) was translated to "磁阻" which sometimes may cause confusion. Here from the definition of the two terms given above, it can be clearly seen the difference between the two notations! It is noteworthy to mention the notation of positive and negative magnetoresistance. Here the positive magnetoresistance refers to the situation where the larger magnetic field leads to larger change of the electrical resistance (i.e. larger deviation percentage), while the negative resistance refers to the opposite situation - the larger the magnetic field, the smaller the deviation percentage. For reference information, see Ref. [27].

- Giant Magnetoresistance

As aforementioned, the discovery of giant magnetoresistance phenomenon brings in wide applications. And here in this section, the physical mechanism behind the giant magnetoresistance will be briefly discussed. In magnetically ordered materials, e.g. the ferromagnetic

materials, there exists magnetic domain in which the electrons spins are will ordered in the same direction. And in such materials, the electrical resistance is crucially influenced by the orientation of the incident electrons as compared to that within the magnetic domain. The detailed reason for the influence of magnetic domain orientation on the electron scattering (thus the electrical resistance) will be given as what follows. For any magnetic domain, since the net orientation of the electron spins point to some specific direction, it indicates that there should exist majority-spin and minority-spin electrons in the domain. However in one specific domain, the Fermi level should be fixed and it is the same for both majority- and minority-spin electrons. This then leads to the difference of density of states (DOS) for majority- and minority-spin electrons - the DOS for minority is higher than that of the majority-spin electrons. To further understand the point here, refer to Fig. 2.5 First of all, the energy of the majority-spin electrons
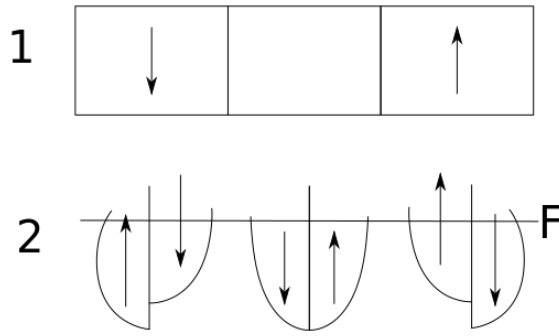

Figure 2.5: The DOS in different magnetic domains, together with that in non-magnetic domain.

is definitely lower than that of the minority-spin electrons (that's just the physical reason why the majority is indeed majority!). Considering the same Fermi level for either majority- or minority-spin electrons, also imagining if we have the same amount of electrons for majority- and minority-spin electrons, then we could instinctively see that the DOS for minority-spin electrons should be higher than that of the majority-spin electrons since the minority-spin electrons tend to be squashed into a smaller 'box'. – The top (analogue to the Fermi level) of the 'box' is the same for both majority- and minority-spin electrons, however for minority-spin electrons, the bottom of the 'box' is lifted thus the overall DOS should be higher, accordingly. More exactly, for transition ferromagnetic metals, the Fermi level of the majority-spin electrons lies in the *sp* band, therefore behaving with no difference to the situation in ferromagnets (the 'ferromagnets' refer to the ferromagnetic materials after the applying of external magnetic field, thus with the same magnetic moment direction overall) and non-magnetic field. However for minority-spin electrons, the *sp* and *d* bands are hybridized, and the Fermi level actually lies in the *d* band. The DOS of the hybridized *spd* band is higher than the *sp* band. The latter explanation is a bit more specific as compared to the previous instinctive understanding. for the difference in DOS between the majority- and minority-spin electrons.

As discussed above, the DOS of minority-spin electrons is higher than that of the majority-spin electrons. Furthermore, it should be noticed that it is actually the DOS around the Fermi level that determines the interaction between the incoming electrons and the electrons within

the magnetic domain. Therefore, the 'effective number' of electrons that can interact with the incoming electrons for both electrons with majority-spin and minority-spin is identical. In another word, it is the DOS around the Fermi level but not the 'majority' or 'minority' that determines the scattering interaction with the incoming electrons. And as aforementioned, the DOS of minority-spin electrons is higher that of the majority ones, thus the scattering effect of minority spin electrons on the incoming electrons is stronger. That's to say, if the incoming electrons are with the spin direction the same with the spin of majority electrons (i.e. opposite to both the net magnetic moment direction and the minority-spin direction), then the incoming electrons 'feel' less scattering therefore the conductivity is higher, as compared to the situation where the spin direction of incoming electrons and the majority-electrons is opposite.

Further information refer to the following link: Click Me! or Click Me!

2.5 General & Advanced Topics

- Majorana Fermion

  Based on the relativistic form of the Shrödinger function – the Dirac function, it can be predicted that the existence of anti-particle, e.g. the anti-particle of electron is the positron. Historically, Dirac thought of the anti-particle of electron predicted by the Dirac equation is just the proton, in his original paper entitled *A theory of electrons and protons*. However, later experiments showed that the anti-particle of electron is actually the positron but not proton, which is much heavier than electron (and positron).

  And the so-called *Majorana Fermion* is such kind of particle of which the anti-particle is just the particle itself. The concept went back to Majorana's suggestion in 1937 that neutral spin-1/2 particles can be described by a real wave function (the Majorana function), and therefore would be indentical to their anti-particle (because the wave function of particle and anti-particle are related by complex conjugate). For details about the Majorana Fermion, refer to the link to Wikipedia here: Click Me

- Weyl Semi-metal

  The Dirac function can be reduced to its half-degree-of-freedom counterpart - the Weyl function. And each 'half' of the Dirac function corresponds to such kind of electrons with specific charality – either left-hand or right-hand as shown in Fig. 2.6.
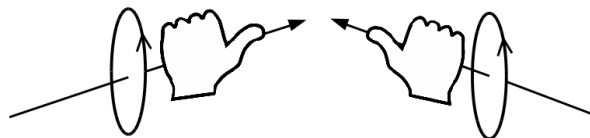

Figure 2.6: The illustration for left-hand and right-hand charality.

Here the charality refers to the relation between the electron spin direction and the translation direction of the electron.

In vacuum, the electrons with left- and right-handed charality often exist in pairs due to the time and space symmetry of the electron wave-function. However, in practical situation, if the electrons with

different charality can be separated, then under the magnetic and electric field that is parallel to each other, electrons with unique charality will be generated continuously. But it was proved in theory, by Nielsen and Ninomiya, that this is not possible in real space, which is the so-called 'No-go' theorem. However, in momentum space, the separation of electrons with different charality can be separated. Nielsen and Ninomiya further pointed that in some crystal materials, if nondegenerate energy bands intercept with each other at some point in k-space, and it happens that the intersection point is somewhere near the Fermi level, then it is possible that electron with unique charality exist in such kind of material, which is then called the *Weyl Semi-metal*. And the corresponding electron with unique charality is then called the *Weyl Fermion*. And the reason why such material is called *semi-metal* is that the density of states (DOS) at the Fermi level is zero – for 'real' metal, the DOS at the Fermi level is obviously non-zero (since otherwise metal will not be conductive).

In *Weyl Semi-metal* material, the *Weyl point* (the k-point where the electrons with unique charality exist) is located in different k-points. And just at those *Weyl points*, electrons with specific charality will be accumulated and the other electrons will be disappear under the magnetic and electric field parallel to each other. The concominant result is that the material will show high negative magnetoresistance. Recent researches have already found some *Weyl Semi-metal* materials such as $Y_2Ir_2O_7$ and $HgCr_2Se_4$, etc. by groups from Nanjing University and Stanford University, etc.

For details information and further reading about the $Weyl Semi-metal$, refer to the materials here following: Material-1 & Material-2.

Chapter 3

Applied Physics

3.1   About Photovoltaic Cells

This section gives some basic problems that are quite often encountered when reading materials about the mechanism and application of photovoltai cells. The fundamental mechanism behind any photovoltaic cells is about the photon excitation. The excited electrons and holes are then separated due to the effect of internal electrical field. Then if the two sides of the photovoltaic cell is connected into circuit, it can produce current accordingly. Therefore, for photovoltaic cells, we want as many photoelectrons as possible to be able to contribute to the current before either radiative or non-radiative decay. And to measure the capability of photo-current transformation, we need to define some certain quantities. The *quantum efficiency* is just such a quantity.

- Quantum Efficiency

  As discussed above, the quantum efficiency is actually defined as the quantity to measure the capability of photo-current transformation. Similar with quantum yield, we also have the internal and external quantum efficiency. Here is the definition for them given by Wikipedia:

  $$EQE = \frac{electrons/sec}{photons/sec} = \frac{current/(charge\,of\,one\,electron)}{(total\ power\ of\ photons)/(energy\ of\ one\ photon)} \tag{3.1}$$

  $$IQE = \frac{electrons/sec}{absorbed\ photons/sec} = \frac{EQE}{1-Reflection-Transmission} \tag{3.2}$$

  It should be pointed out that the notation of 'internal' and 'external' is perhaps more commonly used when talking about the quantum efficiency as compared to quantum yield.

- Multiple exciton generation

  To know about the multiple exciton generation, we may first need to what 'exciton' is. When the photoelectron is excited from the ground state to the excited state, it leaves a hole behind at the ground state level. This uncharged composite is called *exciton*. For conventional solar cell, if the energy of incoming photons is higher than the gap of the material, it can still excite one electron at a time and the excess energy is then dissopated as heat. Now it may become clear what multiple exciton generation means and why it is helpful. Especially in quantum dots solar cells, the multiple exciton generation (MEG) means one photon can excite multiple electrons to the conduction band (taking semiconductor as an example), which, theoretically, could increase the quantum efficiency. The biggest limitation of the MEG process is the short lifetime of the multiexcitons, which restricts its application on

photovoltaic cells. Moreover, it is worth mentioning that the quantum mechanical origin of the MEG process is still under debate, and for details refer to Wikipedia.

Chapter 4

Materials Science

4.1 Nanomaterials Synthesis

In this section, comments about some of the nanomaterials synthesis will be given, and it should be pointed out that no details about the synthesis methods themselves will be provided. For detailed information about the synthesis methods included in current article or those not included, refer to the provided references in this article.

- Sintering of nanoparticles

  To take advantage of the unique properties of bulk nanocrystalline materials, the nanometer range powders have to be densified into parts of certain properties, geometry and size. The commonly used method for compacting nanocrystalline materials into bulk form is sintering. Multiple mechanisms are involved throughout sintering process, namely, evaporation-condensation, surface diffusion, grain boundary diffusion, bulk diffusion, viscous flow and plastic deformation. And it could be easily imagined that during the compacting process, pores will be formed as the sintering processes, therefore the dynamics of both the nanoparticles growth and that of the pores together controls the sintering process of nanoparticles in the pathway to form bulk-sized materials. Here following is given the general relationship between sintering parameters, which concerns the growth of the nanomaterial into its bulk form:

$$\frac{d\rho}{dt} \approx \frac{1}{d^n} exp\left(-\frac{Q}{RT}\right) \tag{4.1}$$

  where n is a constant, ρ is the density, Q is the activation energy for sintering and d is the mean powder particle diameter. And following is the estimation for the pore fraction:

$$\frac{1}{\rho(t)[1-\rho(t)]} \cdot \frac{d\rho}{dt} \approx \frac{1}{r_p(t)} \cdot \frac{1}{d^n} exp\left(-\frac{Q}{RT}\right) \tag{4.2}$$

  where $\rho(t)$ and $r_p(t)$ are the *instantaneous* density and pore radius, respectively. Comprehensively, the Gibbs-Thomson relation gives the driving force, Δp, for the mass transport, expressed as:

$$\Delta p = \frac{2\gamma_b}{d} + \frac{2\gamma}{r} \tag{4.3}$$

  where γ_b is the grain boundary energy, d is the average grain size, γ is the surface free energy, and r is the radius of curvature of pore surfaces. The first term is the grain coarsening tendency, while the second is the sintering driving force. Here is noteworthy to mention that usually sintering process starts at temperature of $0.2-0.4T_{melt}$ for both metals and ceramics and $0.5-0.8T_{melt}$ for conventional powders. All of the

above information can be found in the following material: Introduction to nanomaterials and nanotechnology. To cite this article, refer to the information given in the note (with the same time as given above) stored in Evernote.

Chapter 5

Other General Notes

5.1 About body planes

To make it convenient to talk about our body, several planes are defined bisecting our body two parts. The following graph (Fig. 5.1) illustrates the several defined such planes, In many cases, such terminolgy can also
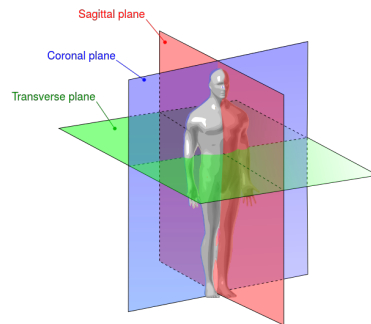

Figure 5.1: Human anatomy planes. Refer to the source: Sagittal plane.

be used in other areas to refer to similar bisecting of an object by the defined planes. Also it should be mentioned that the **sagittal plane** is also sometimes referred to as **median plane** – see the link: Median plane.

Bibliography

[1] K. Dohnalova, A. N. Poddubny, A. A. Prokofiev, W. Boer, C. P. Umesh, J. M. Paulusse, H. Zuihof, and T. Gregorkiewicz. Surface brightens up si quantum dots: direct bandgap-like size-tunable emission. *Light: Science & Applications*, 2:e47, 2013.

[2] R. Q. Zhang, A. D. Sarkar, T. A. Niehaus, and T. Frauenheim. Excited state properties of si quantum dots. *Phys. Status Solidi B*, 2:401–412, 2012.

[3] P. D. J. Calcott, K. J. Nash, L. T. Canham, M. J. Kane, and D. Brumhead. Spectroscopic identification of the luminescence mechanism of highly porous silicon. *J. Lumin*, 57:257–269, 1993.

[4] P. D. J. Calcott, K. J. Nash, L. T. Canham, M. J. Kane, and D. Brumhead. Identification of radiative transitions in highly porous silicon. *L. Phys.: Condens. Matter*, 5:L91–L98, 1993.

[5] S. Takeoka, M. Fujii, and S. Hayashi. Size-dependent photoluminescence from surface-oxidized si nanocrystals in a weak confinement regime. *Phys. Rev. B.*, 62:24, 2000.

[6] N. Shirahata, D. Hirakawa, Y. Masuda, and Y. Sakka. Size-dependent color tuning of efficiently luminescent germanium nanoparticles. *Langmuir*, 29:7401–7410, 2013.

[7] C. Delerue, G. Allan, C. Reynaud, O. Guillois, G. Ledoux, and F. Huisken. multiexponential photoluminescence decay in indirect-gap semiconductor nanocrystals. *Phys. Rev. B.*, 73:235318, 2006.

[8] J. Derr, K. Dunn, D. Riabinina, F. Martin, and M. Chaker. Quantum confinement regime in silicon nanocrystals. *Phys. E.*, 41:668–670, 2009.

[9] J. Linnros, N. Lalic, A. Galeckas, and V. Grivickas. Analysis of the stretched exponential photoluminescence decay from nanometer-sized silicon crystals in sio2. *J. Appl. Phys.*, 86:6128–6134, 1999.

[10] R. Chen. Apparent stretched-exponential luminescence decay in crystalline solids. *J. Lumin*, 102:510–518, 2003.

[11] Y. P. Varshni. Temperature dependence of the energy gap in semiconductors. *Physica*, 34:149–154, 1967.

[12] T. P. Lu, C. H. Du, Y. T. Fang, H. Y. Wu, Y. Jiang, L. Wang, L. G. Dai, H. Q. Jia, W. M. Liu, and H. Chen. Temperature-dependent photoluminescence in light-emitting diodes. *Scient. Rep.*, 4:6131, 2014.

[13] A. L. Erfos and A. L. Erfos. Interband absorption of light in a semiconductor sphere. *Sov. Phys. Semicond.*, 34:772, 1982.

[14] L. E. Brus. On the development of bulk optical properties in small semiconductor crystallites. *J. Lumin.*, 31-2:381–384, 1984.

[15] Y. Kayanuma. Quantum-size effects of interacting electrons and holes in semiconductor microcrystals with spherical shape. *Phys. Rev. B.*, 38:9797–9805, 1988.

[16] M. Dasog, Z. Y. Yang, S. Regli, T. M. Atkins, A. Faramus, M. P. Singh, E. Muthuswamy, S. M. Kauzlarich, R. D. Tilley, and J. G. C. Veinot. Chemical insight into the origin of red and blue photoluminescence arising from freestanding silicon nanocrystals. *ACS. Nano*, 7:2676–2685, 2013.

[17] I. L. Krestnikov, N. N. Ledentsov, A. Hoffmann, D. Bimberg, A. V. Sakharov, W. V. Lundin, A. F. Tsatsul'nikov, A. S. Usikov, and Zh. I. Alferov. Quantum dot origin of luminescence in ingan-gan structures. *Phys. Rev. B.*, 66:155310, 2002.

[18] L. V. Asryan and R. A. Suris. Inhomogeneous line broadening and the threshold current density of a semiconductor quantum dot laser. *Semicond. Sci. Technol.*, 11:554, 1996.

[19] J. E. Chang, P. H. Liao, C. Y. Chien, J. C. Hsu, M. T. Hung, H. T. Chang, S. W. Lee, W. Y. Chen, T. M. Hsu, T. Goerge, and P. W. Li. Matrix and quantum confinement effects on optical and thermal properties of ge quantum dots. *J. Phys. D: Appl. Phys.*, 45:105303, 2012.

[20] G. Gouadec and P. Colomban. Raman spectroscopy of nanomaterials: How spectra relate to disorder, particle size and mechanical properties. *Progr. Cryst. Growth Charact. Mater.*, 53:1–56, 2007.

[21] B. B. Li, D. P. Yu, and S. L. Zhang. Raman spectral study of silicon nanowires. *Phys. Rev. B.*, 59:1645–1648, 1999.

[22] Y. Du, M. S. Zhang, J. Hong, Y. Shen, Q. Chen, and Z. Yin. Structural and optical properties of nanophase zinc oxide. *Appl. Phys. A. Mater. Scienc. Progr.*, 76:171–176, 2003.

[23] Bradley D. Fahlman. *Materials Chemistry.* Springer, Mount Pleasant, MI, USA, 2011.

[24] G. Mie. *Ann. Phys.*, 25:377, 1908.

[25] A. J. Haes, D. A. Stuart, and R. P. Nie, S. Duyne. *Fluoresc.*, 14:355, 2004.

[26] R. L. Kronig and W. G. Penny. *Proc. Roy. Soc.*, 130:499, 1931.

[27] A. E. Kaaouachi, A. Nafidi, and G. Biskupski. *Semicond. Sci. Technol.*, 18:69–74, 2003.